Microfluidic sorting system based on optical force switching

S.-K. Hoi · C. Udalagama · C.-H. Sow · F. Watt · A.A. Bettiol

Abstract We report a versatile, and automatic method for sorting cells and particles in a three dimensional polydimethylsiloxane (PDMS) structure consisting of two cross-microchannels. As microspheres or yeast cells are fed continuously into a lower channel, a line shaped focused laser beam is applied (perpendicular to the direction of flow) at the crossing junction of the two channels. The scattering force of the laser beam was employed to push microparticles matching specific criteria upwards from one channel to another. The force depends on the intrinsic properties of the particles such as their refractive index and size, as well as the laser power and the fluid flow speed. The combination of these parameters gives a tunable selection criterion for the effective and efficient sorting of the particles. The introduction of the cylindrical lens into the optical train allows for simultaneous manipulation of multiple particles which has significantly increased the efficiency and throughput of the sorting. A high aspect ratio microchannel (A.R. = 1.6) was found to enhance the sorting performance of the device. By careful control of the microparticle flow rate, near 100% sorting efficiency was achieved.

PACS 87.80.Cc · 47.15.-x · 47.57.J-

1 Introduction

Usage of microfluidics, which encompasses diverse technological disciplines, has proven to be a versatile and pow-

S.-K. Hoi · C. Udalagama · C.-H. Sow · F. Watt · A.A. Bettiol (✉)
Department of Physics, National University of Singapore,
2 Science Drive 3, Singapore 117542, Singapore
e-mail: phybaa@nus.edu.sg

erful research tool [1, 2]. Compared to conventional large-scale systems, microfabricated devices have a number of advantages for bio-analysis applications, including ultra small reagent (nL) and power consumption, short reaction time and a greater efficiency. For analysis involving biomedical applications, cells are commonly extracted from a larger mixed population for further processing. Efficient manipulation, isolation and sorting of cells or particles is essential for the advancement of microfluid-based life science research and diagnostic platforms. Conventional cell sorting systems could be bulky, costly and manpower intensive. It is therefore worthwhile to develop microfluidic sorting systems to increase both functionality and flexibility on a miniaturized scale. The introduction of a practical, miniature cell particle sorting technique is believed to significantly enhance microfluidic systems for life science research and diagnostics.

Due to the non-invasive and sterile nature of the optical force, coupled with the ability of the optical force to act on inorganic, polymeric and biological particles with minimum degradation, microfluidic sorting using optical force appears to be an attractive option. Optical separation methods do not require any physical coupling between the microchip-bound flow channels and the macroscopic world, giving it a distinct advantage over electrokinetically actuated techniques [3]. Moreover, the application of an electric field could result in complications such as viability of cells or biomolecules, buffer incompatibility, frequent change of voltage settings due to ion depletion and evaporation. Consequently, much research has been focused on the potential of optical sorting techniques in recent years.

Particles sorting with a periodic optical potential energy landscape in a microfluidic system has proved to be one effective method [4–7]. When colloidal particles are driven through the optical landscape, the sample components respond differently to the optical force and this difference in

response leads to particle separation. More recently, Milne et al. demonstrated the separation of four different sized silica beads (2.3 µm, 3.0 µm, 5.3 µm and 6.8 µm) into parallel output flows using an acousto-optically generated potential landscape [8]. Optical chromatography was demonstrated by Hart et al. who introduced a laser that opposed fluid flow in a microfluidic system to achieve optical sample concentration or separation of mixtures of polymer and silica beads [9, 10]. Wang et al. was able to demonstrate an all optical control switch for live cells in a microfluidic fluorescence activated cell sorter (FACS) citing improved buffer medium compatibility when compared with electrokinetic and dielectrophoretic methods [11]. Optical deflection of micro particles with a reconfigurable near field geometry in a total internal reflection microscope system was employed by Marchington et al. to perform passive optical sorting within a microfluidic system [12]. An optical line trap was integrated into a microflow channel chip to achieve fluorescence-based activation and sorting by Applegate et al. [13, 14]. On the other hand, a number of reports present particle sorting using single spot optical tweezers [15–17]. However, the device throughput is limited since manipulation is performed on a cell by cell basis. In addition, inefficient collection of sample components and slow operational flow rate (<100 µm/s) restrict the performance and applicability of many reported optical separation techniques [18–22].

In this paper, we present an alternative optical separation method that can be used to manipulate and sort multiple particles at the same time in a continuous flow environment. The optical sorting method utilizes a three dimensional crossed polymeric microfluidic channel system and an infra-red laser that has been focused onto the device using a low numerical aperture (N.A.) objective lens. Our method relies on the optical scattering force to sort particles according to their size and refractive index. Particle sorting takes place in a relatively small "sorting box" formed by the intersection of two cross channels, thus eliminating the need for long channels or large fractionating arrays. In addition, time-consuming cell tagging or labeling as required in traditional methods (fluorescence activated cell sorting) can be omitted because the separation is mainly based on intrinsic properties of the sample components.

2 Experimental

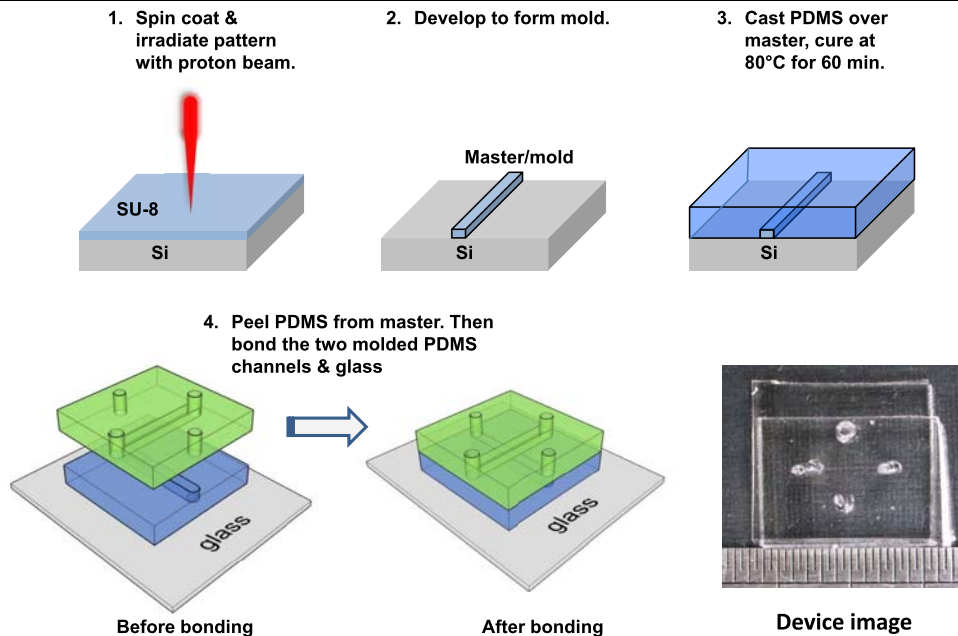### 2.1 Fabrication of microfluidic chips

In order to utilize optical trapping and manipulation for sorting in a microfluidic system, a device needs to be fabricated in a material that is transparent at the wavelengths used for manipulation. The material chosen for our device

was polydimethylsiloxane (PDMS). PDMS is a low cost silicon-based organic polymer that is routinely used in the fabrication of lab-on-a-chip devices by soft lithography. To construct the sorting device, first a master mold was fabricated in a layer of SU-8 photoresist spin coated onto a silicon wafer by using the proton beam writing technique [23]. After development of the SU-8 structure, a hard bake was performed to create a permanent, reusable master that could be used for soft lithography. PDMS molding was carried out to obtain the inverse structure of the master mold. Holes were then punched at the inlets of the device using a Harris Uni-Core punch and the PDMS was trimmed to size. In order to make the final microfluidic device, two pieces of PDMS containing the microchannels were first cleaned using ethanol under sonication and then exposed to air plasma (Plasma Cleaner, Harrick Plasma) for 10 seconds. The two PDMS channels were then bonded to each other such that the two microchannels formed a "tangential contact". Finally, the samples were bonded to a glass microscope slide and heated in an oven at 80°C for 60 minutes. A schematic of the lithographic steps is shown in Fig. 1.
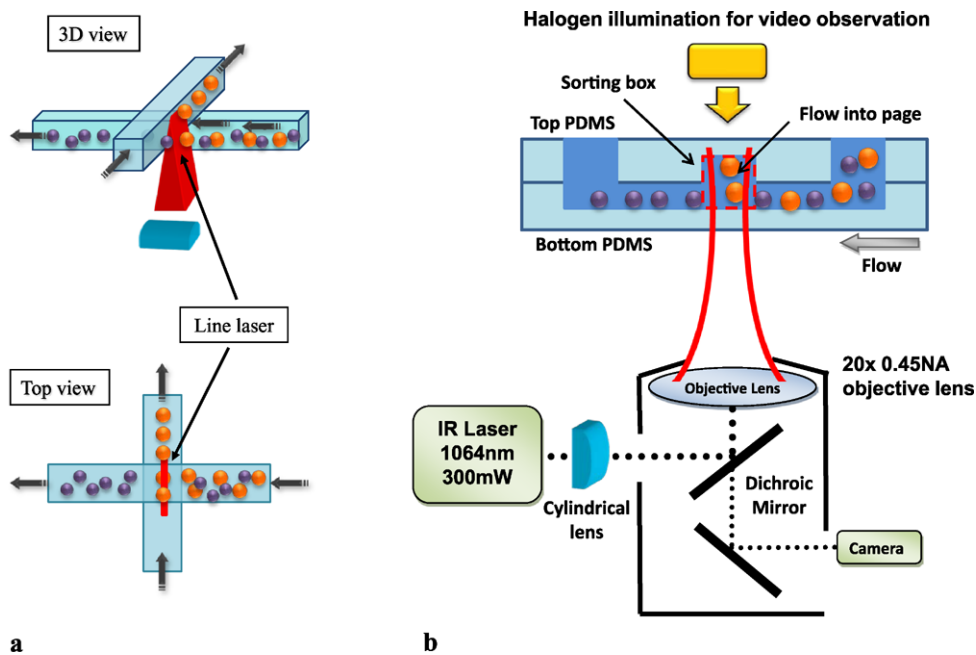
2.2 Experimental procedures

To characterize the microchannel device, an aqueous solution with a mixture of different microparticles was introduced into the lower channel, while deionized water was introduced into the upper channel. At the channel intersection, the flow pattern strongly depends on the aspect ratio of the microchannels [24]. The fluid is driven by a syringe pump (KDS 250) and flows straight through the intersection without there being significant exchange of fluid between the channels, provided the aspect ratio is high (e.g. 1.6). As the microparticles pass by the intersection, they are subjected to a net optical force perpendicular to the direction of flow. Selected particles are strongly pushed upward and switched to the upper channel while the others pass straight through. The difference in the behavior depends on their sensitivity to the optical force. Figure 2 shows the overall concept for a sorting device that switches particles matching specific criteria from the lower channel to the upper channel. A similar 3D cross-channel design has been previously used for magnetic field switching of nanoparticles [25]. Since there is a sustained fluid flow in both the lower and upper channels, when the microparticles move up, they are carried away by the flow automatically. The simple operation of the device allows for an efficient and automated method of sorting microparticles without the need to turn off or translate the laser beam. A single spot focused laser beam was initially used in the system; however, it was slow and inefficient because it was only able to sort particles in the immediate surroundings of the focal point. A larger active sorting area in the cross channel was achieved by introducing a cylindrical

Fig. 1 Processing steps for fabricating the PDMS microchannels and the two level sorting device

1. Spin coat & irradiate pattern with proton beam.
2. Develop to form mold.
3. Cast PDMS over master, cure at 80°C for 60 min.

SU-8
Si

Master/mold
Si

Si

4. Peel PDMS from master. Then bond the two molded PDMS channels & glass

glass

glass

Before bonding

After bonding

Device image

Fig. 2 a Overall concept for an automatic sorting device that switches particles matching specific criteria from the lower channel to the upper channel using line focused laser beam. **b** Schematic of optical sorting microfluidic system. The focused laser was applied at the junction of the two overlapping channels

3D view

Line laser

Top view

a

Halogen illumination for video observation

Sorting box

Top PDMS

Flow into page

Bottom PDMS

Flow

20x 0.45NA objective lens

Objective Lens

IR Laser 1064nm 300mW

Cylindrical lens

Dichroic Mirror

Camera

b

lens into the optical train to spread the beam into a line focus [20]. The line shaped focused laser beam spanned across the "sorting box" (50 µm). This modification to the optical system significantly increased the throughput of the sorting process by allowing for the simultaneous manipulation of multiple particles.

In order to observe the operation of the particle sorting device, the chip was mounted on an inverted microscope (Nikon TE2000-U). A dichroic mirror was used to reflect the laser beam (DPSS laser SUWTECH, 1064 nm—300 mW) towards the back aperture of the objective lens

(20 × 0.45 N.A. Nikon) while allowing for the illumination light and particle image to pass through to a CCD video camera connected to a PC. Using this setup, the operation of the device could be observed in real time. Silica, polystyrene (PS) microspheres and yeast cells (deionized water as carrier) ranging in size from 1.5 µm to 6 µm (Polyscience, Inc. and Bangslab, USA) were used in the study. The IR laser power at the back aperture of the objective lens was measured to be 100 mW for experiments involving yeast cells and 300 mW for experiments involving PS and silica microspheres.

3 Results and discussion

The operation of the microfluidic optical sorting device may be viewed in the video footage provided in the supplementary material. In order to understand its operation one must consider the forces acting on the microparticles as they move through the intersection of the two channels. The force on a particle in an optical trap is the net result of a scattering force and a gradient force. When microparticles first encounter the focused laser spot, the gradient force acts to rapidly slow them down. In order for this to occur, the gradient force must be sufficiently large to overcome the drag force. For very low Reynolds numbers (Re $\ll$ 1), the inertial forces can be neglected and the drag force on a uniform sphere moving through a viscous fluid can be approximated by

$$F_{\text{Drag}} = 6\pi\eta v a \tag{1}$$

where η is the fluid viscosity, v is the velocity of the sphere with respect to the flowing fluid, and a is radius of the sphere. The interplay between the optical gradient force and the fluid drag force determines the first sorting criterion. If the velocity of the microparticle is too large, then for a given laser power and objective lens numerical aperture there is not enough force to stop the particles. In addition to being stopped by the optical gradient force, a scattering force will act on the microparticle in a direction perpendicular to the fluid flow. The strength of the scattering force depends on the refractive index, size and intensity of input laser [26, 27]. Therefore particles that are larger in size or higher in refractive index are more readily deflected by the optical field. For objective lenses that have a relatively low numerical aperture, the scattering force dominates over the gradient force resulting in the particle being pushed by the laser rather than being trapped at the focus. The deflection of some of the microparticles by the scattering force is the main mechanism for sorting in the microfluidic device. Microparticles that meet specific criteria primarily determined by their size, refractive index and the laser power can be separated from a mixture by being pushed by a focused laser into an upper channel.

Various experiments were performed to characterize the sorting efficiency of the three dimensional microfluidic channel system. In order for the sorting experiments to be performed reliably, we first made sure that the fluid in upper and lower microchannels did not mix. If mixing did occur then microparticles, regardless of their physical or optical properties, could move automatically from lower to upper channel. It was found that the aspect ratio of the microchannels plays an important role in determining the flow at the intersection. At the intersection, a fluid element has two possible paths that it can follow. The fluid can travel straight through the intersection with a cross sectional area of ($h \times w$) or it can move from the lower channel to the upper channel by going through a cross section area of ($w \times w$) where w is the width of the channel and h is its height. Since the fluid follows a path that offers the least viscous resistance, channels with high aspect ratio should result in the least amount of mixing between the upper and lower microchannel. In order to study the influence of the microchannel aspect ratio, two devices were fabricated. Microchannels of 30 µm height and 50 µm width (aspect ratio A.R. = 0.6) were first used, followed by 40 µm height and 25 µm width channels (aspect ratio A.R. = 1.6).

Figure 3a shows the trajectories of yeast cells using a device with low aspect ratio microchannels (A.R. = 0.6) in the absence of a laser line. Yeast cells and spores (small yeast cell with diameter <3 µm) are represented by crosses and lines respectively. Figure 3b and c shows the trajectories of the smaller and larger cells respectively in the presence of laser line. Due to the laminar flow of the microfluidic system, the tracks of the separated cells form a band which corresponds to the optical trap line. From these trajectories, we observe that the sorting mechanism does not necessar-
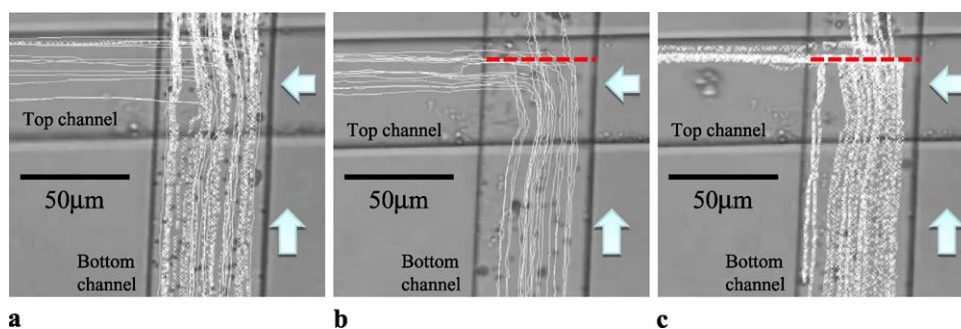

Fig. 3 a Trajectories of yeast cells with laser turned off. *Solid lines* represent small cells and *crosses* represent big cells. Big cells (*cross*, with diameter >3 µm) kept flowing in the bottom channel while some of the smaller cell (*lines*, with diameter <3 µm) may escape from the flow and switch to the upper channel. **b–c** Trajectories of small yeast cells (**b**) and big yeast cells (**c**) with presence of laser respectively. The *dotted lines* indicate the position of line laser. The sorting box was $50 \times 50 \times 60$ µm^3 in size. Laser power ~100 mW. The cells were moving at speeds ~120 µm/s. The white arrows show the direction of fluid flow

ily need to be an optical effect when the aspect ratio of the channel is 0.6. Figure 3a shows that even without the presence of laser beam, yeast spores (diameter <3 µm) can be switched to the upper channel. Moreover, some of the yeast spores shown in Fig. 3b were switched before encountering the trap line. The laser line is however effective in switching larger cells from the lower microchannel to the upper microchannel as can be seen in Fig. 3c.

To enhance the sorting efficiency, a high aspect ratio microchannel (A.R. = 1.6) device was adopted. Microsphere mixtures of either different size or different refractive index (keeping the other factors fixed) were used to investigate the dependence of the sorting efficiency on the particles' sizes, refractive index and flow speed. The separation of PS microspheres with a diameter of 5.6 µm and 1.5 µm is shown in Fig. 4. The optical force acting on the large PS spheres (square) is greater than the force acting smaller spheres (triangles). When the microparticles come into contact with the line laser (dashed box), the large sphere are stopped and pushed to the upper channel while the small spheres pass straight through. As a result, the large and small spheres can be successfully separated and collected at two different outlets. Figure 5a and b show the trajectories (solid lines) of polystyrene (PS) spheres with a diameter of 1.5 µm and 5.6 µm respectively in the presence of a line laser (dashed box). The particle flow speed was varied from 10 µm/s to 750 µm/s, under a constant laser power of 300 mW. The smaller PS spheres were not switched by the laser while larger PS spheres were switched efficiently when they encountered the line laser at an optimum flow speed. Figure 5c

and d represent respectively the trajectories of PS spheres and silica spheres of the same size (4.5 µm fluorescent PS sphere, $n = 1.59$ and 4.5 µm silica spheres, $n = 1.43$). As we can see in Fig. 5c, the PS spheres' trajectories formed a
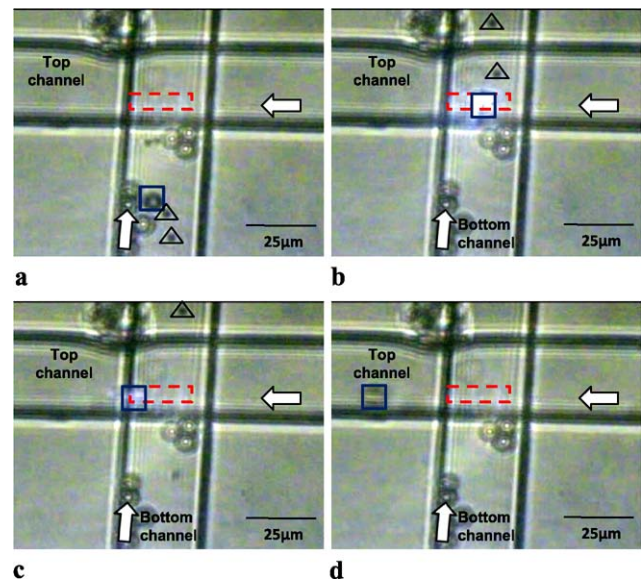
**Fig. 4** Sequential images of PS spheres when passing through the intersection. **a** Large (*square*, 5.6 µm) and small (*triangles*, 1.5 µm) PS spheres initially flowing in the bottom channel. **b–c** when encounter the line laser (*dashed box*), the large sphere was stopped and being push to upper channel while the small spheres pass straight through. **d** The large and small spheres with same refractive index was successfully separated and is readily collected at two different outlets. The *white arrows* show the direction of fluid flow

Fig. 5 Trajectories of PS spheres with a diameter of **a** 1.5 µm and **b** 5.6 µm respectively. The speed of the particles is ∼250 µm/s. The *dashed white box* indicates the position of line laser and the *white arrows* show the direction of fluid flow. Due to slight misalignment of the laser, the line focus did not span the entire width of the channels. The sorting box was $25 \times 25 \times 80$ µm^3 in size and the laser power was ∼300 mW. Trajectories of PS spheres with diameter of **c** 4.5 µm and silica beads with a diameter of **d** 4.5 µm. The speed of the particles is ∼300 µm/s
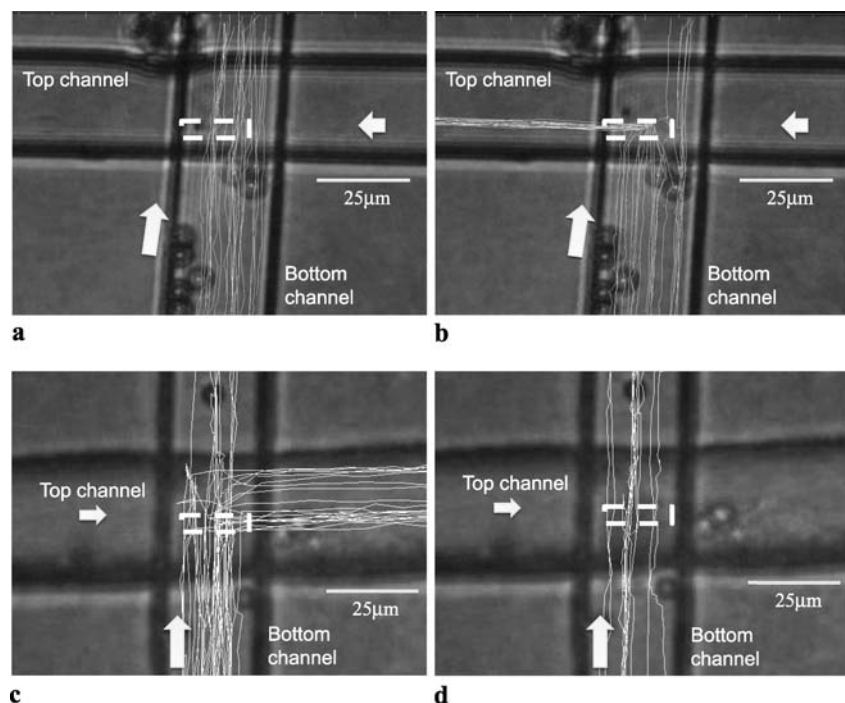
Fig. 6 **a** Switching percentage for mixtures of PS spheres with a diameter of 5.6 μm, 1.5 μm and the FOM. **b** Switching percentage for a mixture of PS spheres with a diameter of 4.5 μm and silica beads with a diameter of 4.5 μm. Laser power ∼300 mW
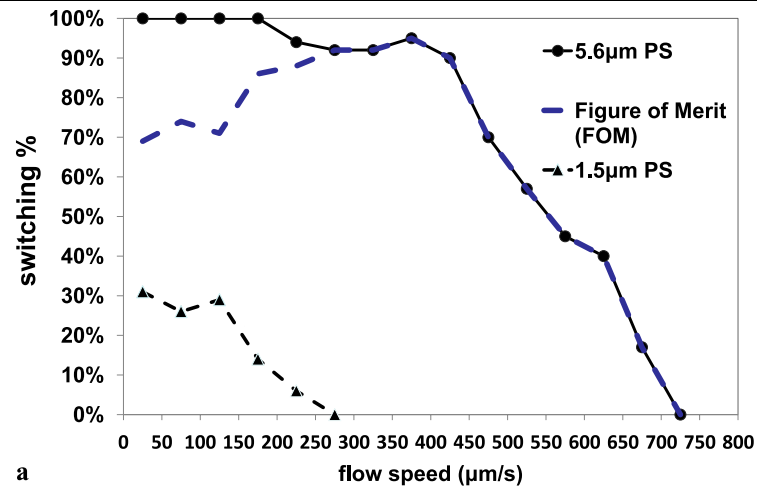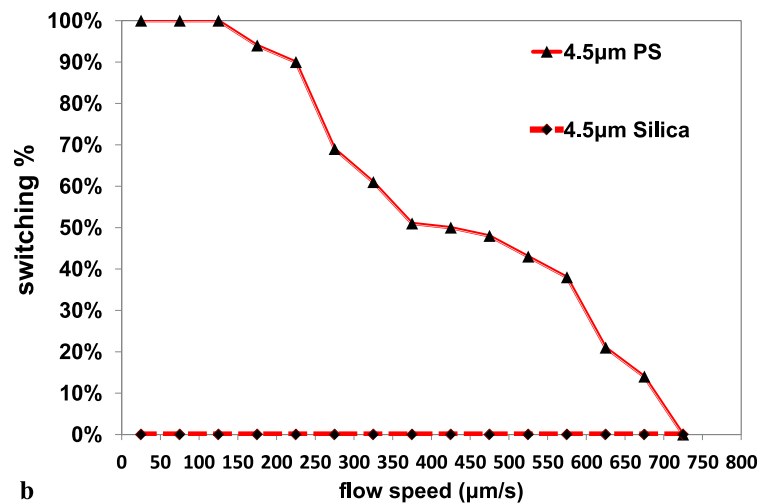
broader band in the upper channel. This is because when the PS spheres are moving too fast, the trapping of the spheres is less effective and hence the spheres do not stay in the line. However, the spheres are still pushed to the upper channel of the sorting box and switched when their speed in the original direction is slowed to zero. On the other hand, the optical scattering force that acted on the silica spheres was not strong enough for them to be switched from the lower channel to the upper channel. Thus, as shown in Fig. 5d, no silica beads were found in the upper channel. As a result, effective separation of two different types of microspheres can be achieved.

The performance of the sorting system can be illustrated by means of Fig. 6. It shows the variation of particles' switching percentage as a function of flow speed, taken from statistical analysis of more than 2000 microspheres. From the plots in Fig. 6a, it can be seen that larger spheres are sorted more efficiently than smaller one. PS spheres with a diameter of 5.6 μm were switched with a high efficiently (>90%) when the flow rates do not exceed 425 μm/s. The percentage of switching starts to drop grad-

ually as the flow speed is increased. Beyond 725 μm/s, no PS spheres are switched since the flow speed of the spheres was too fast. The optical stopping force required to overcome the viscous drag force can be estimated from Fig. 6. Using (1), we deduce that the optical force required to stop the PS spheres with a diameter of 5.6 μm from its original flow direction ranged from 9 pN to 38 pN. The maximum in the stopping force is attributed to the narrowest point of the focused beam which contains the strongest electric field gradient.

PS spheres with a diameter of 1.5 μm were sorted less efficiently as compared to larger sized spheres. The maximum switching percentage is 30% and drops to zero when the flow speed exceeds 275 μm/s. The maximum optical stopping force that acts on these smaller PS spheres was deduced to be 4 pN. This is consistent with the fact that the optical force acting on the larger spheres is stronger than the force acting on smaller spheres. In order to measure the sorting efficiency for the PS spheres mixture, an outcome-based figure of merit (FOM) was used. We denote "A" as the percentage of PS spheres with a diameter of 5.6 μm

that were switched successfully by the laser beam over the whole sphere with a diameter of 5.6 µm in the mixed solution; "B" as the percentage of PS spheres with a diameter of 1.5 µm that were switched over all the spheres with a diameter of 1.5 µm in the mixture. The FOM is defined as $(A - B)$. The plot in Fig. 6a presents the experimental results for this efficiency FOM, as a function of flow speed. The separation of particles utilizes the balance between optical and fluidic forces. Hence, the efficiency FOM reaches a maximum if the flow speed is optimized for the laser power. As shown in Fig. 6a, the FOM for spheres was about 70% at a speed of 25 µm/s and rose gradually as flow speed increased. In the speed range of 275–425 µm/s, the FOM became >90% and started to drop beyond 425 µm/s. The optimum flow speed for maximum sorting efficiency depends on the laser power and can be increased by increasing the laser power.

A second mixture containing PS spheres and silica spheres of the same size (4.5 µm fluorescent PS sphere, $n = 1.59$ and 4.5 µm silica spheres, $n = 1.43$) was studied. PS spheres can be separated easily from the mixture because silica spheres were not switched for all flow rates (Fig. 6b). This is due to the weaker force that acts on these spheres that have a lower refractive index [26, 27]. PS spheres with a diameter of 4.5 µm were switched efficiently (>90%) with flow speed not exceeding 225 µm/s. The switching percentage dropped gradually and finally to zero at 725 µm/s. The silica spheres of the same size were not switched for all flow speeds. The optical stopping force that acts on PS spheres was 5–30 pN. From the experimental results and comparing the influences of the two factors (refractive index and size), we can conclude that the influence of refractive index on optical scattering force is significantly stronger than the particle's size.

4 Conclusion

We developed a non-invasive, versatile and efficient method for sorting cells and colloidal particles within a microfluidic system. The proposed system and method excluded the time-consuming process for sample labeling and promises the ability to produce final samples with a high degree of purity. The three-dimensional sorting channel geometry provides a convenient platform to selectively sort particles automatically using optical force. The experiments performed show that standard operations for microfluidic devices such as fractional removal, separation, concentration, sorting, and fluid/particle handling are all possible with an appropriate optical field strength and flow rate. Sorting particles/cells of different size or refractive index does not require a new channel configuration or modified dimensions. The only adjustment is to properly control the flow rate or laser power.

The optical sorting method can be easily scaled to fluidic networks of greater complexity by multiplexing a high power laser beam to multiple sorting boxes on a chip. This will enable a higher throughput and parallel sorting.

References

1. S. Haeberle, R. Zengerle, Lab Chip **7**, 1094–1110 (2007)
2. H.C. Hunt, J.S. Wilkinson, Microfluid Nanofluid **4**, 53–79 (2008)
3. L. Wang, L.A. Flanagan, N.L. Jeon, E. Monuki, A.P. Lee, Lab Chip **7**, 1114–1120 (2007)
4. M.P. MacDonald, G.C. Spalding, K. Dholakia, Nature **426**, 421–424 (2003)
5. K. Ladavac, K. Kasza, D.G. Grier, Phys. Rev. E **70**, 010901 (2004)
6. A.M. Lacasta, J.M. Sancho, A.H. Romero, K. Lindenberg, Phys. Rev. Lett. **94**, 160601 (2005)
7. R.L. Smith, G.C. Spalding, K. Dholakia, M. MacDonald, J. Opt. A, Pure Appl. Opt. **9**, 134–138 (2007)
8. G. Milne, D. Rhodes, M. MacDonald, K. Dholakia, Opt. Lett. **32**, 1144–1146 (2007)
9. S.J. Hart, A.V. Terray, J. Arnold, T.A. Leski, Opt. Express **15**(5), 2724–2731 (2007)
10. S.J. Hart, A.V. Terray, J. Arnold, Appl. Phys. Lett. **91**, 171121 (2007)
11. M.M. Wang, E. Tu, D.E. Raymond, J.M. Yang, H. Zhang, N. Hagen, B. Dees, E.M. Mercer, A.H. Forster, I. Kariv, P.J. Marchand, W.F. Butler, Nat. Biotech. **23**, 83 (2005)
12. R.F. Marchington, M. Mazilu, S. Kuriakose, V.G. Chavez, P.J. Reece, T.F. Krauss, M. Gu, K. Dholakia, Opt. Express **16**(6), 3712–3726 (2008)
13. R. Applegate Jr., J. Squier, T. Vestad, J. Oakey, D. Marr, Opt. Express **12**, 4390–4398 (2004)
14. R.W. Applegate, J. Squier, T. Vestad, J. Oakey, D.W.M. Marr, P. Bado, M.A. Dugan, A.A. Said, Lab Chip **6**, 422–426 (2006)
15. J. Oakey, J. Allely, D.W.M. Marr, Biotechnol. Prog. **18**, 1439–1442 (2002)
16. J. Enger, M. Goksor, K. Ramser, P. Hagberg, D. Hanstorp, Lab Chip **4**, 196–200 (2004)
17. C.C. Lin, A. Chen, C.H. Lin, Biomed. Microdevices **10**, 55–63 (2008)
18. S.C. Chapin, V. Germain, E.R. Dufresne, Opt. Express **14**(26), 13095 (2006)
19. Y.Y. Sun, X.C. Yuan, L.S. Ong, J. Bu, S.W. Zhu, R. Liu, Appl. Phys. Lett. **90**, 031107 (2007)
20. F.C. Cheong, C.H. Sow, A.T.S. Wee, P. Shao, A.A. Bettiol, J.A. Van Kan, F. Watt, Appl. Phys. B (Lasers Opt.) **83**(1), 121–125 (2006)
21. K. Grujic, O.G. Helleso, J.P. Hole, J.S. Wilkinson, Opt. Express **13**, 1–7 (2005)
22. I. Ricardez-Vargas, P. Rodriguez-Montero, R. Ramos-Garcia, K. Volke-Sepulveda, Appl. Phys. Lett. **88**, 121116 (2006)
23. J.A. van Kan, L.P. Wang, P.G. Shao, A.A. Bettiol, F. Watt, Nucl. Instrum. Methods Phys. Res. B **260**, 353–356 (2007)
24. R.F. Ismagilov, D. Rosmarin, P.J.A. Kenis, D.T. Chiu, W. Zhang, H.A. Stone, G.M. Whitesides, Anal. Chem. **73**, 4682–4687 (2001)
25. A.H. Latham, A.N. Tarpara, M.E. Williams, Anal. Chem. **79**, 5746–5752 (2007)
26. A. Ashkin, Appl. Phys. Lett. **19**, 283–285 (1971)
27. A. Ashkin, J.M. Dziedzic, J.E. Bjorkholm, S. Chu, Opt. Lett. **11**, 288–290 (1986)